

# We are IntechOpen, the world's leading publisher of Open Access books Built by scientists, for scientists

4,800

Open access books available

122,000

International authors and editors

135M

Downloads

Our authors are among the

154

Countries delivered to

TOP 1%

most cited scientists

12.2%

Contributors from top 500 universities



WEB OF SCIENCE™

Selection of our books indexed in the Book Citation Index  
in Web of Science™ Core Collection (BKCI)

Interested in publishing with us?  
Contact [book.department@intechopen.com](mailto:book.department@intechopen.com)

Numbers displayed above are based on latest data collected.

For more information visit [www.intechopen.com](http://www.intechopen.com)



# Computational Fluid Dynamic Simulations of Natural Convection in Ventilated Facades

A. Gagliano, F. Patania, A. Ferlito, F. Nocera and A. Galesi  
*Department of Industrial and Mechanics Engineering, Faculty of Engineering,  
University of Catania,  
Italy*

## 1. Introduction

The European Directive 2002/91/EC (Energy Performance of Buildings) aims to achieve minimum standards on the energy performance of new buildings and existing buildings that are subject to major renovation.

To evaluate the energy performance of a building is necessary to calculate the energy required to satisfy the various services related to the standard usage of the building.

In order to achieve the minimum standards for energy certification should be an approach to design alternative to the traditional one which allows to reduce significantly the building's energy requirements maintaining the level of indoor comfort.

The energy needs of the building depend on the efficiency of envelope: when it was not designed and constructed correctly, the heat fluxes through the structures (vertical, horizontal, transparent, opaque) cause a large increase in final energy consumption.

The heat exchanges depend on the temperature difference between the inner and the outer faces of the boundary element (horizontal or vertical) and the thermal resistance of the material (or combination of materials) that constitute the envelope and the contribute of solar radiation.

In summer, especially during the days with high values of temperature and solar radiation, the building envelope should be designed and constructed so as to ensure adequate environmental conditions for thermal comfort in the indoor environment, even in absence of conditioning systems.

## 2. The ventilated facade system

The ventilated facade is a multi-layer coating system that was born in Northern Europe in order to have an envelope that combine aesthetic aspect with a strong positive valence valuable in terms of insulation and energy saving.

Subsequently the deep technological innovations have improved the system and it has found large use in many other countries with increasing recognition.

Today the use of ventilated structures in new buildings is a widely used solution in architecture because it provides both high energy savings and elevated aesthetic - formal contents.

Contemporary architecture shows an increased interest in the building envelope, such as evidenced by the words of Herzog: "*It is meaningful to talk about of the building envelope as a skin "and not merely a "protection", something that "breathes", which governs the weather and environmental conditions between the inside and outside, similar to that of humans. "*"

Among the examples of structures that use the system of the ventilated facade is possible to cite the Jewish Museum in Berlin of Libeskind, the Gehry's Guggenheim Museum in Bilbao and the Theatre La Scala in Milan built by Botta.

The use of ventilated walls and roof is also a useful application in case of restoration and renovation of old buildings. There is a significant number of legislative measures to promote increases in volume when they produce an improvement in the energy behavior of the building.

From a structural viewpoint, a ventilated facade presents an outer facing attached to the outer wall of the building through a structure of vertical and horizontal aluminum alloy or other high-tech materials, so as to leave between the outer and inner wall surfaces a "blade" of air. Often the gap is partially occupied by a layer of insulating material attached to the wall of the building, to form a "coat" protected from atmospheric agents by the presence of the external face of the ventilated facade.

Each of the layers that make up the ventilated wall has a very specific function (see fig.1):

1. The *outer coating* is designed to protect the building structure from atmospheric agents, as well as being the finishing element that confers the building aesthetic character. Among the coating systems can be distinguished those made of "traditional materials" and those made using "innovative materials" (metal alloys or plastics). Recently found increasing use materials already widely used in traditional as ceramic or brick, produced and implemented in a completely innovative way, such as assembly of prefabricated modular panels attached by mechanical means without recourse traditional mortars. This application has many advantages such as ease of installation and maintenance, both favored by the possibility of intervention on each slab.
2. The *resistant layer*, which can either be made of load-bearing walls (made of bricks, blocks of lightweight concrete or brick) or traditional masonry (brick or stone, mixed) to be recovered and been rebuilt, is that to which is secured by an anchoring system properly sized, the outer coating.
3. The *insulating layer* has the task to cancel the thermal bridges, forming an effective barrier to heat loss. The uneven distribution of surface temperatures, especially in modern building which is in fact discontinuous in shape and heterogeneity of materials, determines areas of concentration of heat flux. This problem is drastically reduced by the system of insulation coat, which surrounds the building with a cover of uniform thermal resistance with significant energy benefits.
4. The *anchoring structure* (substructure), usually made of aluminum alloy is directly anchored to the inner wall using special anchors. Since its function is to support the weight of the external coating, the choice of the kind of structure and the sizing must take into account such factors as the weight of the coating, the characteristics of the surrounding environment and the climate of the area (wind, rain, etc.).
5. The *air gap* between the resistant element and the coating is the layer within which generates an upward movement of air, the chimney effect, triggered by heating of the external coating.

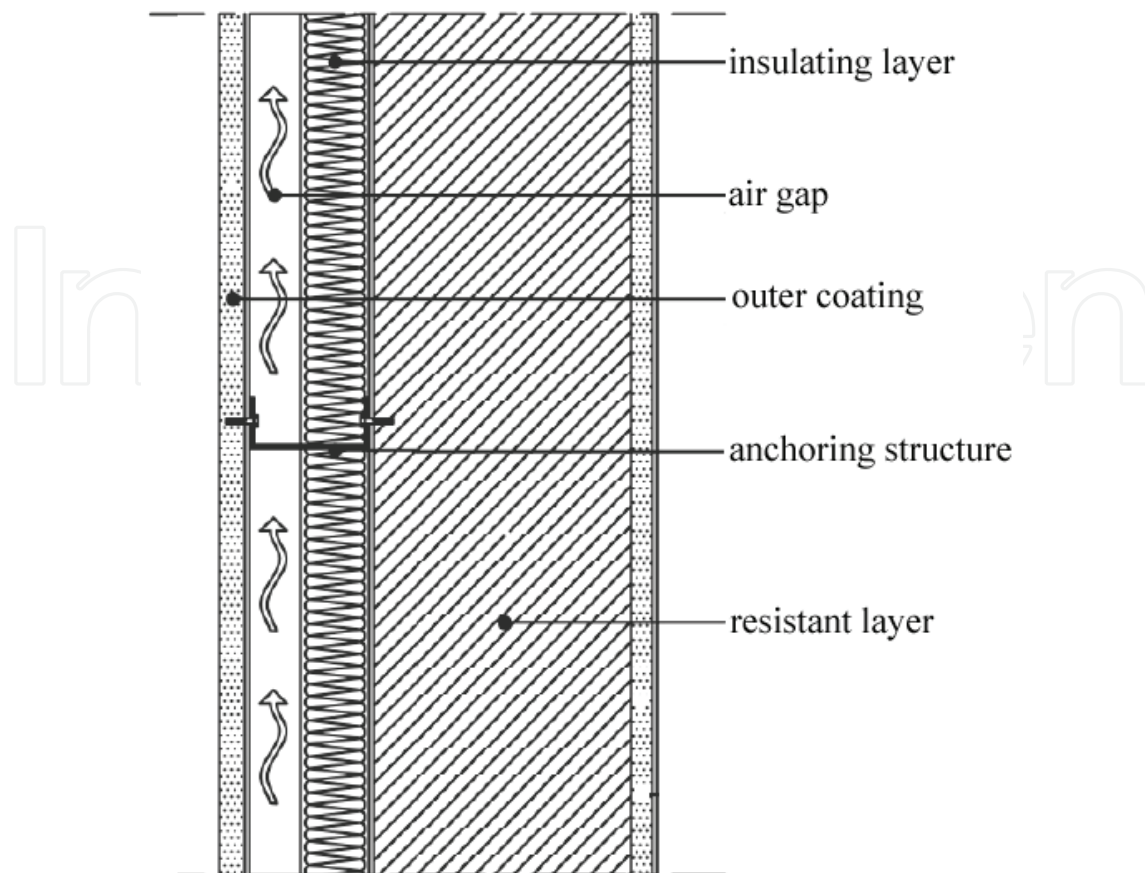


Fig. 1. Ventilated facade - Section

From a thermo-fluid dynamic viewpoint, during summer period, the outside air entering in the cavity, is heated by contact with the external face at a higher temperature due to the incident solar radiation. This causes a change in air density inside the air gap and the formation of an upward movement that produces a benefit especially in the summer (see fig.2 a) because it eliminates some of the heat that is not reflected by coating.

During the winter season (see fig.2 b) the solar radiation incident on the structure is much smaller than in summer and the air outside and inside the gap have approximately the same temperature, resulting in a very reduced stack effect. The movement of air allows the evacuation of water vapor decreasing the possibility of interstitial condensation.

The study of the energy performance of ventilated walls requires a CFD analysis of the airflow within the cavity both in cases where it is due only to thermal and pressure gradients (chimney effect), and when it is induced by the propulsion of fans (forced convection).

This thermo-fluid dynamics analysis of the ventilated cavity is a very complex procedure, which requires a very detailed knowledge of the geometry of the system and thermo physical properties of materials.

These elements, in addition to the difficulties in the determination of the convective coefficients the approximations necessary for the values used for the boundary conditions can drastically reduce the reliability of CFD methods based on numerical solution of this problem.

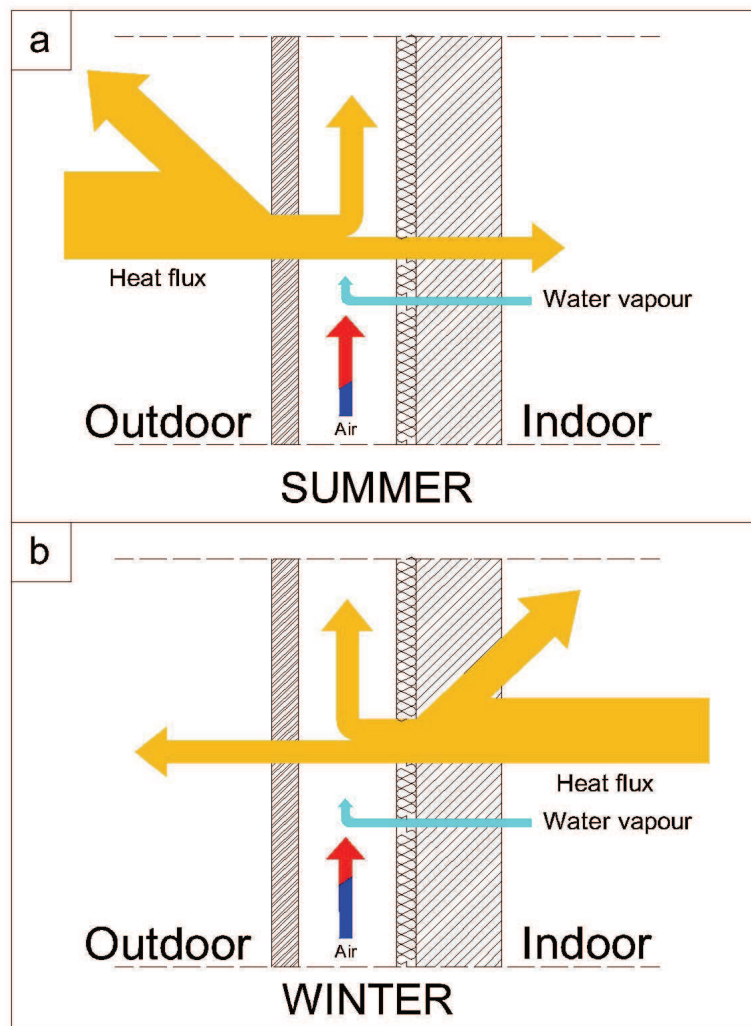


Fig. 2. Summer (a) and winter (b) functioning of ventilated facade

### 3. The calculation model

Authors have developed a calculation model to evaluate the energy performances of the ventilated façade. The first critical step of the numerical solution of a thermo-fluid dynamics problem is the identification of an appropriate physical model able to describe the real problem.

The best choice is to use a physical model not excessively complex.

Therefore have been made two very important choices:

- The use of a two-dimensional geometric model;
- The introduction of the hypothesis of stationarity.

The ventilated walls object of the study have been schematized as a two-dimensional system (see fig.3) consisting of two slabs, one internal and one external, which delimit a duct in which the air flows. The structure has length " $L$ " and thickness of the air gap " $d$ ". The Cartesian reference system has been placed with the origin at the beginning of the ventilation duct, oriented with the  $y$ -axis in the direction of motion.

At the base and upper part of the facade there are two air vents, with height " $a$ ", which connect the ventilated cavity with the external environment.

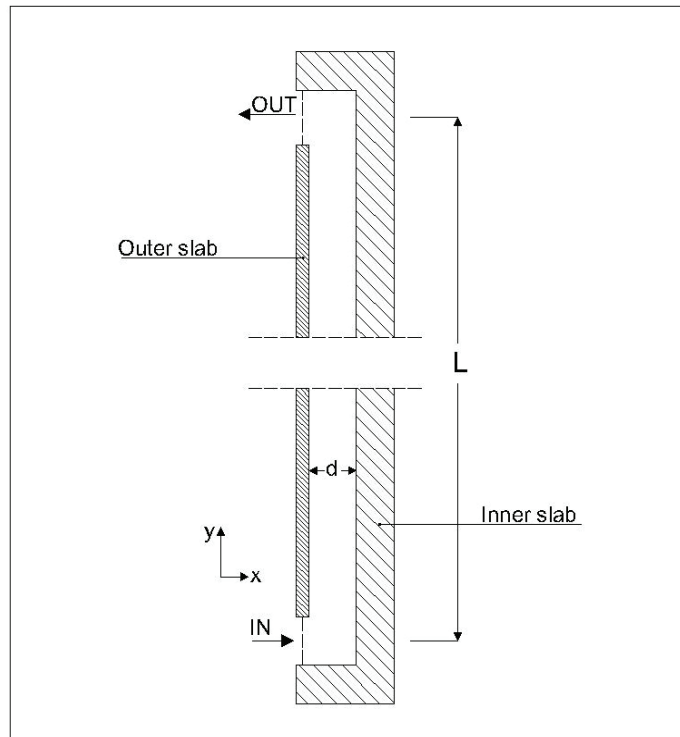


Fig. 3. Bi-dimensional model of ventilated facade

The second critical step in the numerical resolution of the problem is the characterization of the heat exchanges.

The ventilated structure is characterized by the simultaneous presence of three types of heat transfer: convection, conduction and radiation (see fig. 4).

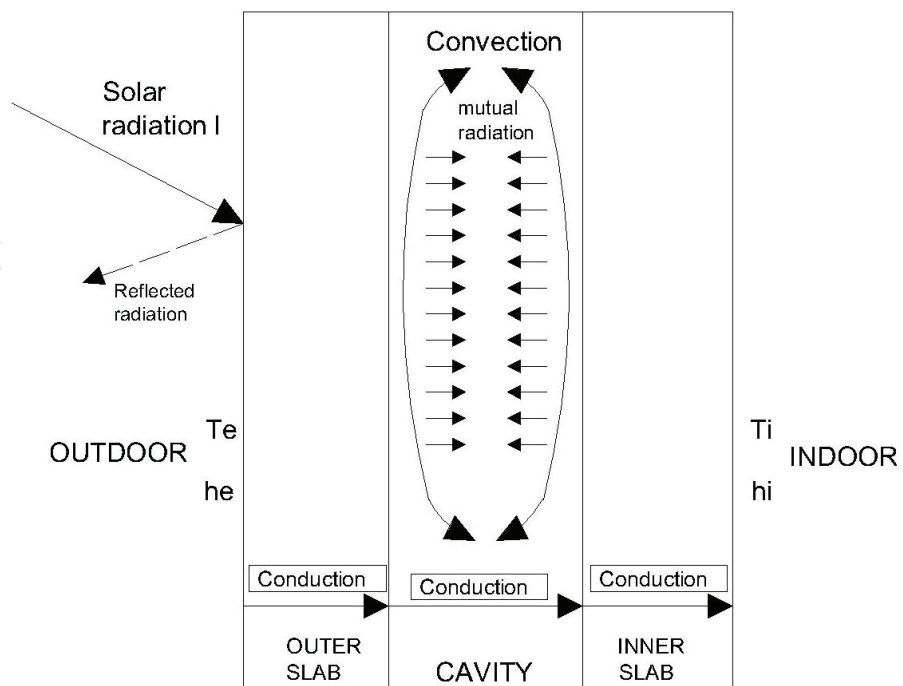


Fig. 4. Heat exchanges

The transmission of heat will be caused by:

- convective and radiative exchanges between the external environment and the exterior surface of the coating;
- conductive heat exchange through the walls of the duct;
- radiative exchange between the two slabs delimiting the air gap;
- convective heat exchange between these slabs and the air circulating inside the channel;
- convective and radiative exchanges between the indoor and the intrados of the inner wall.

The conductive heat transfer through the inner and outer walls has been characterized by the conductive thermal resistance defined by:

$$R_{cond} = \sum_i \frac{s_i}{\lambda_i} \quad (1)$$

where  $s_i$  and  $\lambda_i$  and are respectively the thickness and thermal conductivity of the  $i$ -th layer of the wall.

In steady-state analysis, the convective and the radiative heat transfers within the ventilated cavity can be represented with an acceptable level of accuracy considering two thermal resistances,  $r_1$  and  $r_2$ , expressed by the following equations :

$$r_1 = r_A \frac{R_0}{r_A + r_B + R_0} \quad \text{and} \quad r_2 = r_B \frac{R_0}{r_A + r_B + R_0} \quad (2)$$

where  $r_A$  and  $r_B$  are the thermal resistances due to the convective exchange between the fluid and the two garments (A and B respectively), while the thermal resistance  $R_0$  characterizes the mutual radiative exchange between the two inner sides of the ventilated duct.

The thermal resistance  $R_0$  has been expressed by the following equation:

$$R_0 = \frac{1 - e_1}{A_1 \cdot e_1} + \frac{1}{A_1 \cdot F_{12}} + \frac{1 - e_2}{A_2 \cdot e_2} \quad (3)$$

where  $A_1$  and  $A_2$  are the areas of the two slabs,  $F_{12}$  is the view factor between the two parallel surfaces, while  $e_1$  and  $e_2$  are the emissivity coefficient on both sides of the duct.

The convective thermal resistance ( $r_A$  and  $r_B$ ) inside the ventilated channel have been assessed using the relationship of Gnielinski valid for Reynolds numbers (Re) higher than 2300.

Using this model it is possible to calculate the Nusselt number of fluids in transient conditions from linear to turbulent flow which can be expressed as:

$$Nu_0 = \frac{\frac{\xi}{8} (Re - 1000) Pr}{1 + 12.7 \sqrt{\frac{\xi}{8}} (Pr^{2/3} - 1)} \quad (4)$$

Where  $Pr$  is the Prandtl number and  $\xi$  represents the friction coefficient, calculated by means of the correlation discovered by Petukhov reported below:

$$\xi = \frac{1}{(1.82 \log \text{Re} - 1.64)^2} \quad (5)$$

The influence of temperature has been considered with the introduction of the following relation:

$$Nu = Nu_0 \left( \frac{T_m}{T_w} \right)^{0.36} \quad (6)$$

where  $T_m$  is the mean temperature of the fluid in the cavity and  $T_w$  is the temperature of the wall of the ventilated duct.

The convective thermal resistances ( $r_A$  and  $r_B$ ) at inner and outer surfaces of the duct have been calculated by the equations:

$$r_A = Nu_0 \left( \frac{T_m}{T_{wA}} \right)^{0.36} \frac{\lambda}{D_h} \quad \text{and} \quad r_B = Nu_0 \left( \frac{T_m}{T_{wB}} \right)^{0.36} \frac{\lambda}{D_h} \quad (7)$$

where  $D_h$  is the hydraulic diameter defined as:

$$D_h = 2 \frac{dL}{(d+L)} \quad (8)$$

The third step of the numerical solution of the problem is the definition of energy and motions equations for the flow of the air inside a cavity.

The steady state energy balance has been applied to a control volume, which represents the whole of modules with two opaque layers separated by the air channel.

The time-averaged Navier-Stokes equations of motion for steady, compressible flow can be written as :

- Conservation of mass (continuity) in  $i^{\text{th}}$  direction

$$\frac{\partial}{\partial t} + \nabla \cdot (\rho \vec{v}) = 0 \quad (9)$$

Where  $\rho$  is the air density and  $\vec{v}$  the velocity vector

- Conservation of momentum in  $i^{\text{th}}$  direction

$$\frac{\partial}{\partial t} (\rho \vec{v}) + \nabla (\rho \vec{v} \vec{v}) = -\nabla p + \nabla (\vec{\tau}) + \rho \vec{g} + \vec{F} \quad (10)$$

where  $p$  is the static pressure,  $\vec{\tau}$  is the shear stress tensor, while  $\rho \vec{g}$  and  $\vec{F}$  represent respectively the body and the external forces.

- Conservation of energy

$$\frac{\partial}{\partial t} (\rho E) + \nabla \cdot [\vec{v} (\rho E + p)] = \nabla \cdot \left[ k_{\text{eff}} \nabla T - \sum_i h_i \vec{j}_i + (\vec{\tau}_{\text{eff}} \cdot \vec{v}) \right] + S_h \quad (11)$$

where  $k_{\text{eff}}$  is the effective conductivity.



The first three terms in the right side of the equation represent energy exchanges due to convection, conduction and viscous dissipation, while the term  $S_h$  includes the contributions of the heat produced by chemical reactions.

The two transport equations for the standard  $k$ -epsilon model, also derived from the Navier-Stokes equations, can be written as follows:

- Turbulent kinetic energy ( $k$ -equation)

$$\frac{\partial}{\partial t}(\rho k) + \frac{\partial}{\partial x_i}(\rho k u_i) = \frac{\partial}{\partial x_j} \left[ \left( \mu + \frac{\mu_t}{\sigma_k} \right) \frac{\partial k}{\partial x_j} \right] + P_k + P_b - \rho \varepsilon - Y_M + S_k \quad (12)$$

- Kinetic energy of turbulence dissipation ( $\varepsilon$ -equation)

$$\frac{\partial}{\partial t}(\rho \varepsilon) + \frac{\partial}{\partial x_i}(\rho \varepsilon u_i) = \frac{\partial}{\partial x_j} \left[ \left( \mu + \frac{\mu_t}{\sigma_k} \right) \frac{\partial \varepsilon}{\partial x_j} \right] + C_{1\varepsilon} \frac{\varepsilon}{k} (P_k + C_{3\varepsilon} P_b) - C_{2\varepsilon} \rho \frac{\varepsilon^2}{k} + S_\varepsilon \quad (13)$$

Where the turbulent viscosity has been expressed as follow:

$$\mu_t = \rho C_\mu \frac{k^2}{\varepsilon} \quad (14)$$

The production of turbulent kinetic energy  $P_k$  can be expressed by the equation:

$$P_k = \mu_t S^2 \quad (15)$$

where the term  $S$  is the average strain tensor expressed by the relation:

$$S \equiv \sqrt{2S_{ij}S_{ij}} \quad (16)$$

The effect of buoyancy forces is expressed by the following equation:

$$P_b = \beta g_i \frac{\mu_t}{Pr_t} \frac{\partial T}{\partial x_i} \quad (17)$$

where  $Pr_t$  is the turbulent Prandtl number and  $g_i$  is the component of gravity vector in the  $i$ -th direction.

The constants have the following default values [1]:

$$C_{1\varepsilon}=1,44, C_{2\varepsilon}=1,92; C_{3\varepsilon}=1; C_\mu=0,09; \sigma_\varepsilon=1,3 \text{ and } \sigma_k=1,0.$$

The governing equations have been solved using the *finite volumes* method that is particularly suitable for the integration of partial differential equations. These equations are integrated in a control volume with boundary conditions imposed at the borders.

The interior of this domain is divided in many elementary volumes linked by mathematical relationships between adjacent volumes so is possible to solve the Navier-Stokes equations with the aid of a computer code.

#### 4. Generation of the computational grid

The solution of differential equations using numerical methods requires computational grids, commonly called meshes. The computational grid is a decomposition of the problem space into elementary domains.

The simplicity of the domain of study has allowed the use of a structured grid characterized by the exclusive presence of 2D quadrilateral elements and a regular connectivity. The computational grids used to simulate the behavior of air in ventilated cavities in this study are simple quadrilateral mesh with a pitch of 0.5 cm in all directions.

The resolution of the numerical problem in the regions close to the solid walls, have a significant impact on the reliability of the results obtained through numerical simulations, because in these areas arise the phenomena of vorticity and turbulence requiring the use of specific wall functions.

The analysis was performed used the method called *enhanced wall* treatment, which involves the division of the computational domain in two regions: one where is predominant the effect of turbulence and another in which prevails the effect of viscosity, depending on of the value assumed by the turbulent Reynolds number, expressed using the following equation:

$$\text{Re}_y = \frac{\rho y \sqrt{k}}{\mu} \quad (18)$$

where  $y$  is the normal distance between the solid wall and the centers of the cell while  $k$  represents the turbulent kinetic energy in correspondence the wall.

## 5. Boundary conditions

In mathematics, a boundary condition is a requirement that the solution of a differential equation must satisfy on the margins of its domain. Differential equation admits an infinite number of solutions and often to fix some additional conditions is needed to identify a particular solution, which will also be unique if the equation satisfies certain regularity assumptions.

The inlet temperature  $T_0$  has been imposed coincident with the external temperature  $T_e$ , while the pressure at the same section is equal to the atmospheric pressure  $p_0 = \text{patm}$ .

The outlet pressure  $p_L$  has been determined using the relationship:

$$p_L = p_0 - \rho g L \quad (19)$$

The pressure drop located at the openings connecting the ventilated cavity to the external environment have been evaluated using the following equation:

$$\Delta p = k \rho \frac{v^2}{2} \quad (20)$$

where  $v$  and  $\rho$  are the average velocity and density of the fluid while  $k$  is the localized loss coefficient, obtained experimentally, which assumes values  $k_0 = 0.5$  and  $k_L = 1$  respectively at the inlet and the outlet sections.

The determination of turbulent flow parameters,  $k$  and  $\varepsilon$ , has previously required the calculation of turbulent intensity  $Tu$ , which has been calculated using an empirical correlation specifically adopted for flows in pipes:

$$Tu = \left( \frac{v'}{\bar{v}} \right)^2 = 0.16 \left( \text{Re}_{D_h} \right)^{-1/8} \quad (21)$$

The turbulent kinetic energy  $k$  has been calculated using the equation:

$$k = \frac{3}{2}(\bar{v}Tu)^2 \quad (22)$$

where  $\bar{v}$  is the average velocity of flow.

The rate of turbulent kinetic energy dissipation  $\varepsilon$  has been calculated using the formula:

$$\varepsilon = C_\mu^{\frac{3}{4}} \frac{k^{\frac{3}{2}}}{l} \quad (23)$$

where  $C_\mu$  is a constant characteristic of the empirical  $k$ - $\varepsilon$  turbulence model that assumes the value of 0.01, while  $l$  is the turbulent length scale.

An approximate relationship between the physical size of the pipe is the following:

$$l = 0.07L \quad (24)$$

where  $L$  is the characteristic size of the duct, which in the case of channels with non-circular section is coincident with the hydraulic diameter ( $L = Dh$ )

The boundary conditions for natural convection case are summarized in Table 1.

	$y = 0$	$y = L$	$x = 0$	$x = d$
<b>p</b>	$p = p_0$	$p = p_0 - \rho_0 g L$	-	-
<b>T</b>	$T = T_0$	-	$T = T_1$	$T = T_2$
<b>v</b>	-	-	$v = 0$	$v = 0$
<b>r</b>	-	-	$r = r_1$	$r = r_2$
<b>k</b>	$k = k_0 = \frac{3}{2} T u_0 v_0^2$	-	$k = 0$	$k = 0$
<b><math>\varepsilon</math></b>	$\varepsilon = \varepsilon_0 = C_\mu^{\frac{3}{4}} \frac{k_0^{\frac{3}{2}}}{T u_0}$	-	$\varepsilon = 2 (\mu/\rho) \left( \frac{C_\mu}{\kappa} \right) \left( \frac{\partial k_0^{3/2}}{\mu x_w} \right)$	$\varepsilon = 2 (\mu/\rho) \left( \frac{C_\mu}{\kappa} \right) \left( \frac{\partial k_0^{3/2}}{\mu x_w} \right)$

Table 1. Boundary conditions for natural convection case:

In the case of forced convection it has been defined the inlet velocity of the fluid while the boundary conditions imposed on other elements of the geometry of the channel are coincident with those used for the study carried out under natural convection.

## 6. The study sample

The studied case involved the analysis of a module with a length  $L = 6$  m, and a depth  $D = 1$  m. The characteristic size of the ventilated duct have been chosen according with the values proposed by the reference in literature in order to obtain the best energy performance for this kind of structure.

The Authors have studied four types of ventilated facade called respectively: P1, P2, P3 and P4.

	Layer	Material	Width (m)	$\rho$ (kgm <sup>-3</sup> )	$\lambda$ (Wm <sup>-1</sup> K <sup>-1</sup> )
<b>Facade P1</b> $R_{\text{tnv}} = 1.855$ m <sup>2</sup> KW <sup>-1</sup>	1 (Ext)	Brick slabs	0.045	800	0.30
	2	Air (ventilation duct)	0.10	-	0.56
	3	Rigid fibreglass panels	0.04	100	0.038
	4	Cement mortar	0.015	2000	1.40
	5	Brick in hollow blocks	0.18	1600	0.59
	6 (Int)	Lime mortar and cement plastering	0.015	1800	0.90
<b>Facade P2</b> $R_{\text{tnv}} = 1.855$ m <sup>2</sup> KW <sup>-1</sup>	1 (Ext)	Slabs of ceramics	0.013	2700	1.00
	2	Air (ventilation duct)	0.10	-	0.56
	3	Rigid fibreglass panels	0.03	100	0.038
	4	Cement mortar	0.015	2000	1.40
	5	Brick in hollow blocks	0.19	1200	0.43
	6 (Int)	Lime mortar and cement plastering	0.015	1800	0.90
<b>Facade P3</b> $R_{\text{tnv}} = 1.855$ m <sup>2</sup> KW <sup>-1</sup>	1 (Ext)	Cement fibred reinforced panels	0.05	315	0.92
	2	Air (ventilation duct)	0.10	-	0.56
	3	Rigid fibreglass panels	0.03	100	0.038
	4	Cement mortar	0.015	2000	1.40
	5	Brick in hollow blocks of concrete	0.14	1100	0.35
	6 (Int)	Lime mortar and cement plastering	0.015	1800	0.90
<b>Facade P4</b> $R_{\text{tnv}} = 1.855$ m <sup>2</sup> KW <sup>-1</sup>	1 (Ext)	Aluminum	0.001	2700	220
	2	Vermiculite	0.026	90	0.08
	3	Aluminum	0.001	2700	220
	4	Air (ventilation duct)	0.10	-	0.56
	5	Cement mortar	0.01	1800	0.70
	6	Poroton Block	0.2	1600	0.17
	7 (Int)	Lime mortar and cement plastering	0.015	1800	0.70

Table 2. Thermophysical characteristics of unventilated roofs.

Thermo-physical characteristics and geometry (thickness  $d$ , density  $\rho$ , solar absorptivity  $\alpha$ , and conductivity  $\lambda$ ) of the four structures are showed in Table 2. The four samples of facade have been chosen with the same value of thermal resistance ( $R_{\text{nv}}=1,855\text{m}^2\text{kW}^{-1}$ ) but different external surface coating:

- facade *P1* has a brick exterior coating;

- facade *P2* has a coating of ceramic tiles;
- facade *P3* has a coating of cement fibred reinforced panels;
- facade *P4* has an external coating made of insulated panels in vermiculite covered with aluminum on both sides.

In all the studied cases, the outer layer is anchored to a supporting structure made of brick blocks. The facades *P1*, *P2* and *P3* present the insulating layer, consisting of a rigid fibreglass panel with a thickness of 4 cm, placed in the inner slab, while in the case of the facade *P4* the coating panel also acts as insulation layer.

The ventilation openings that connect the ventilated cavity with the external environment are placed at the base and at the upper part of facade and have a size of 20 cm x 100 cm

The friction factors and heat transfer coefficients are assumed to be constant along the duct.

Generally, the roughness value of the air duct is assumed to be quite high in order to take into account the presence of supports inside the air duct. Obviously this parameter is not uniform throughout the whole structure but it is realistic in the portion of the channel that is not affected by the presence of supporting elements.

Therefore the sensitivity analysis for this parameter have been performed.

The roughness  $b$  has been varied from 0,005 m up to 0,03 m. This sensitive analysis didn't show significant variations both for the velocity profiles and for the energy performance of the ventilated facade. The value of roughness has been estimated as  $b = 0,02$  m.

The solar absorptivity coefficient  $a$  has been defined constant because its difference between the three studied cases is about from 0.02 up to 0.04, so it involves only a few hundredths of temperature degrees changes in the temperature sun-air  $T_{as}$ . According to the studies in references the solar absorption coefficient has been fixed in  $a = 0,8$ .

Thermal resistances of inner and outer surfaces have been defined respectively  $r_i = 0.13$   $m^2kW^{-1}$  and  $r_e = 0.04$   $m^2kW^{-1}$ .

## 7. Results and discussions

The authors have studied the behavior of the four types of facades, both in case of natural ventilation and in the case of forced ventilation of the air in the duct.

For the study of a typical summer situation have been considered the following reference conditions:

- External temperature:  $T_e = T_0 = 301$  K;
- Indoor temperature:  $T_i = 297$  K;
- Incident solar radiation:  $I = 400$  W/m<sup>2</sup>.

The modeling of the real system has been performed using the computer code "Fluent" and the pre-processor "Gambit".

The convergence criterion requires that the maximum relative difference between two consecutive iterations for each local variable is less than  $10^{-3}$ .

Convergence has been generally obtained with a number of iterations, which varies from case to case, but always between 800 and 1200 iterations.

### 7.1 Natural ventilation

Initially has been studied the behavior of the ventilated facade system in natural ventilation, with the motion of air in the cavity caused by thermal and pressure gradients.

Figures 5 to 12 show the velocity and temperature profiles obtained for the four facades.

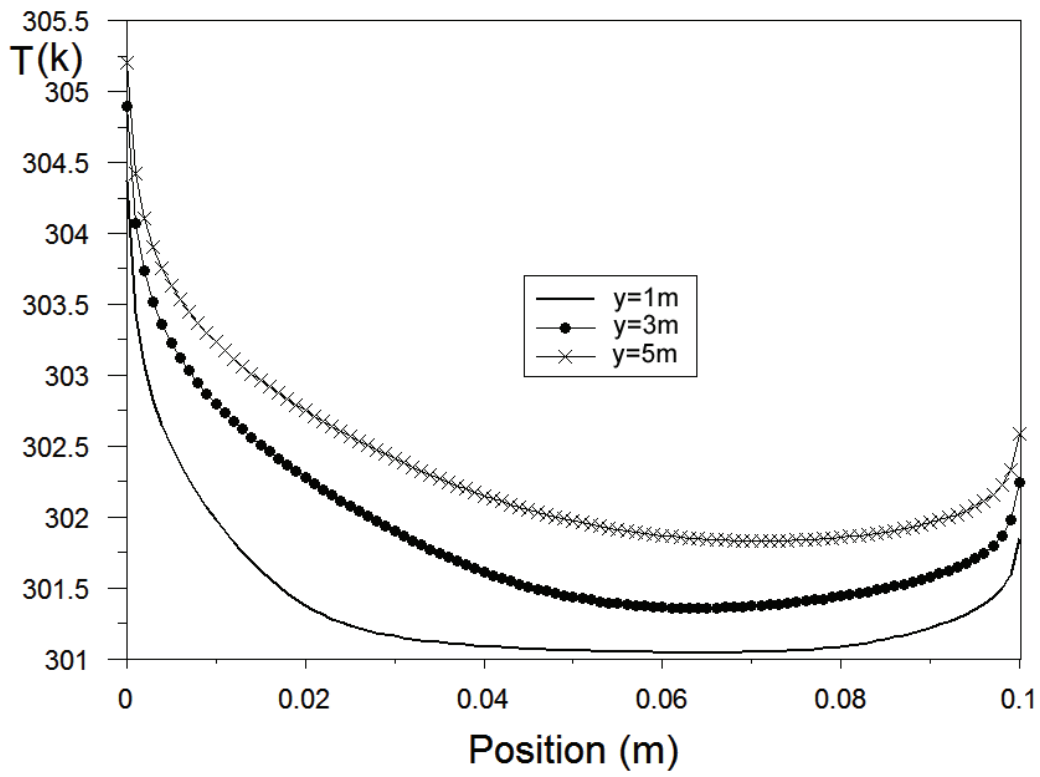


Fig. 5. Facade P1- Temperature profiles ( $L=6\text{ m}$ ,  $d=0.1\text{ m}$ ,  $T_e=301\text{ K}$ ,  $I=400\text{ W/m}^2$ )

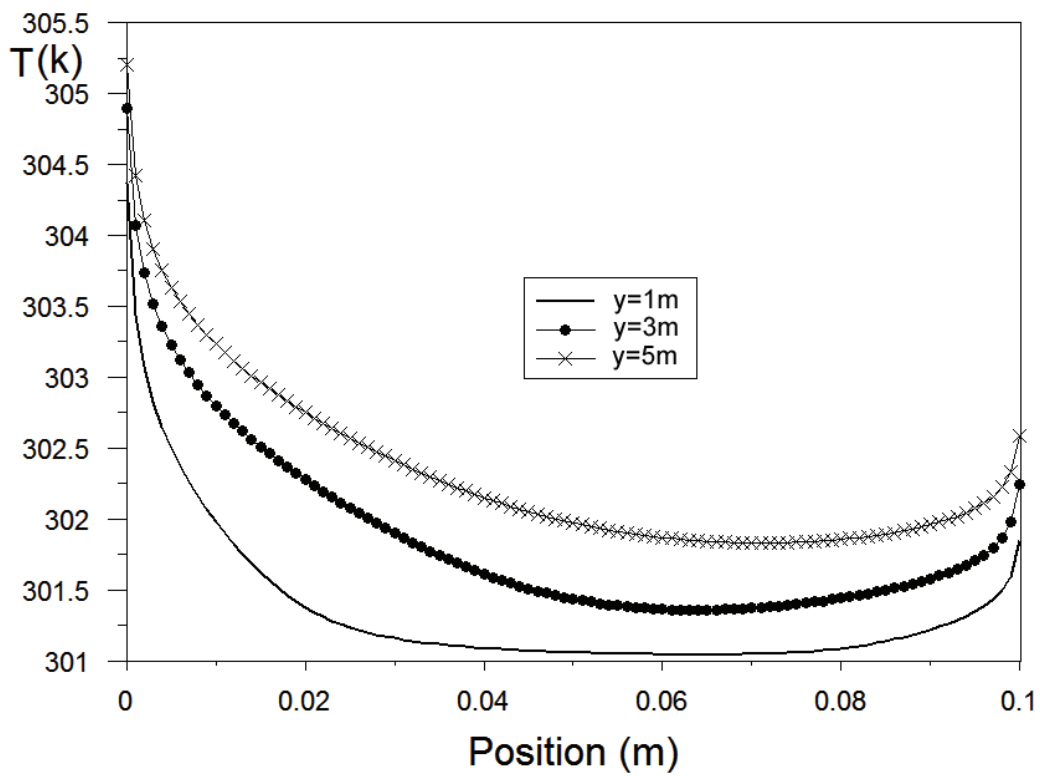


Fig. 6. Facade P2- Temperature profiles ( $L=6\text{ m}$ ,  $d=0.1\text{ m}$ ,  $T_e=301\text{ K}$ ,  $I=400\text{ W/m}^2$ )

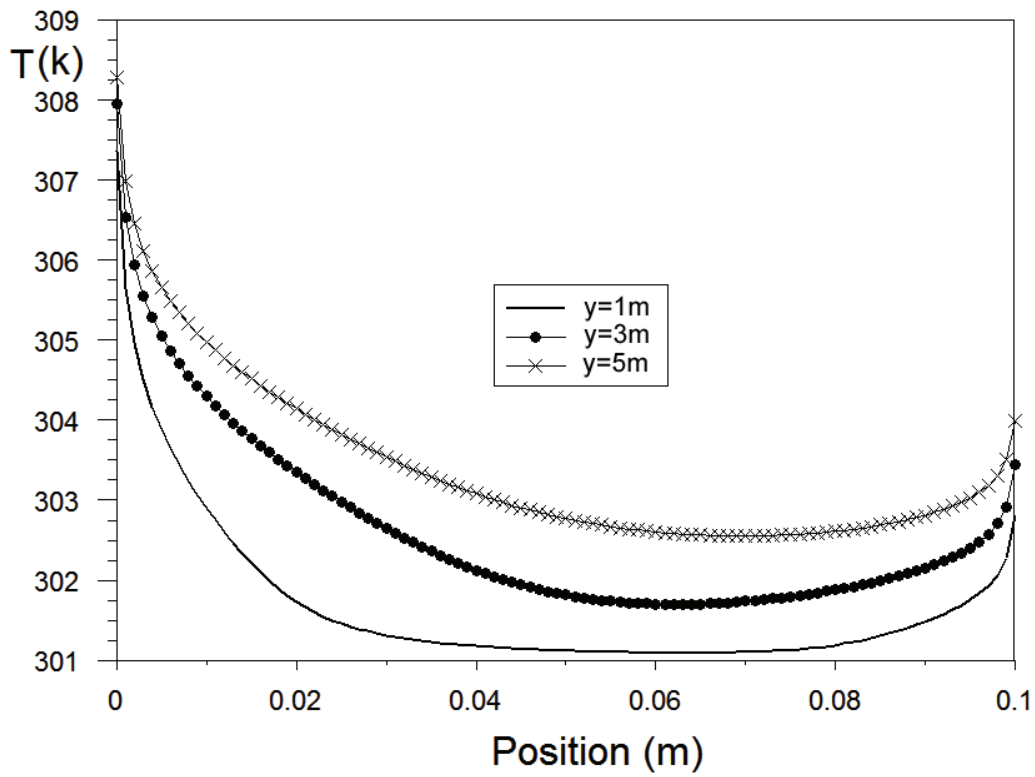


Fig. 7. Facade P3- Temperature profiles ( $L=6$  m,  $d=0.1$  m,  $T_e=301$  K,  $I=400W/m^2$ )

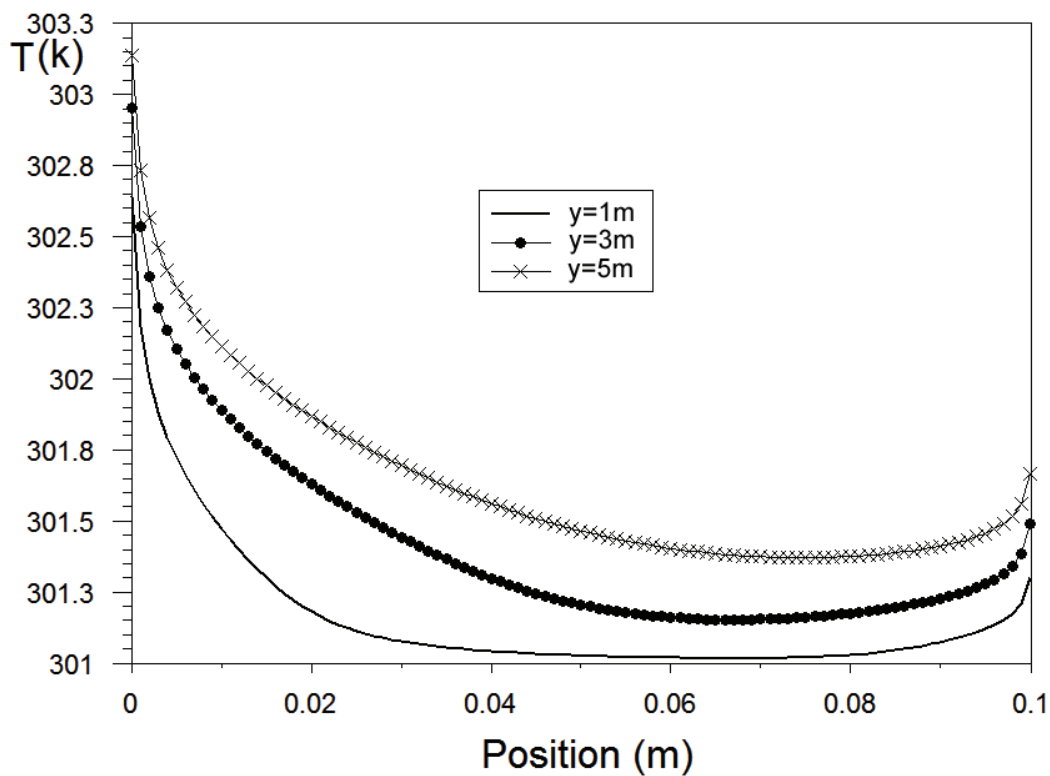


Fig. 8. Facade P4- Temperature profiles ( $L=6$  m,  $d=0.1$  m,  $T_e=301$  K,  $I=400W/m^2$ )

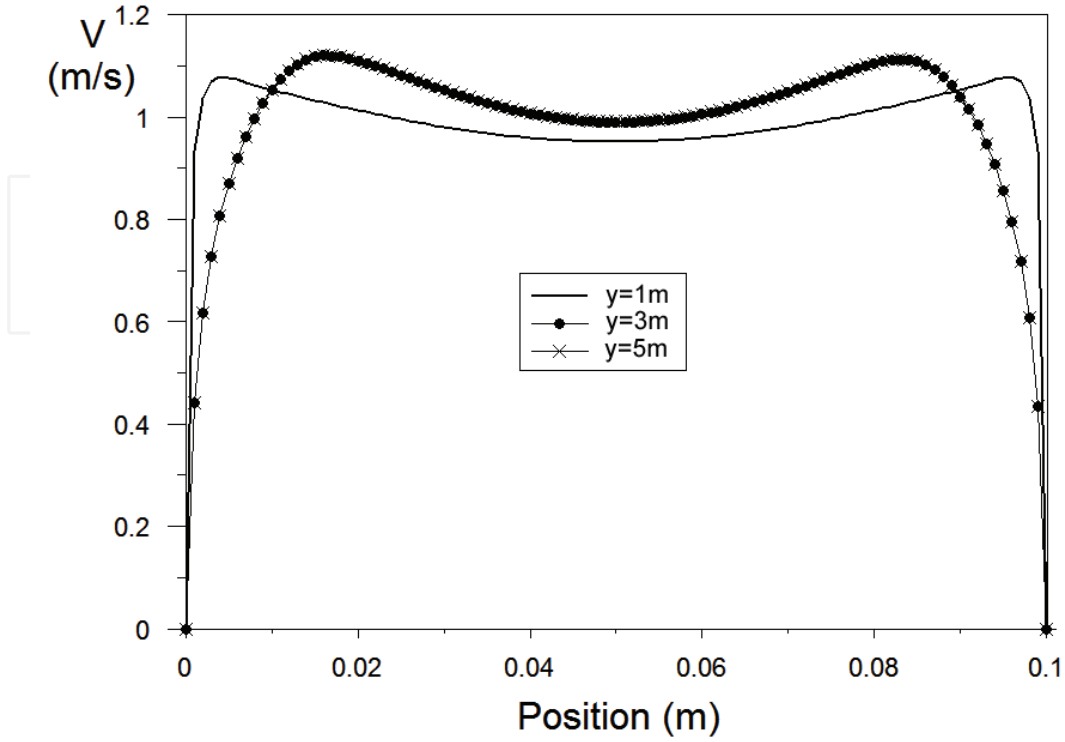


Fig. 9. Facade P1- Velocity profiles ( $L=6$  m,  $d=0.1$  m,  $T_e=301$  K,  $I=400W/m^2$ )

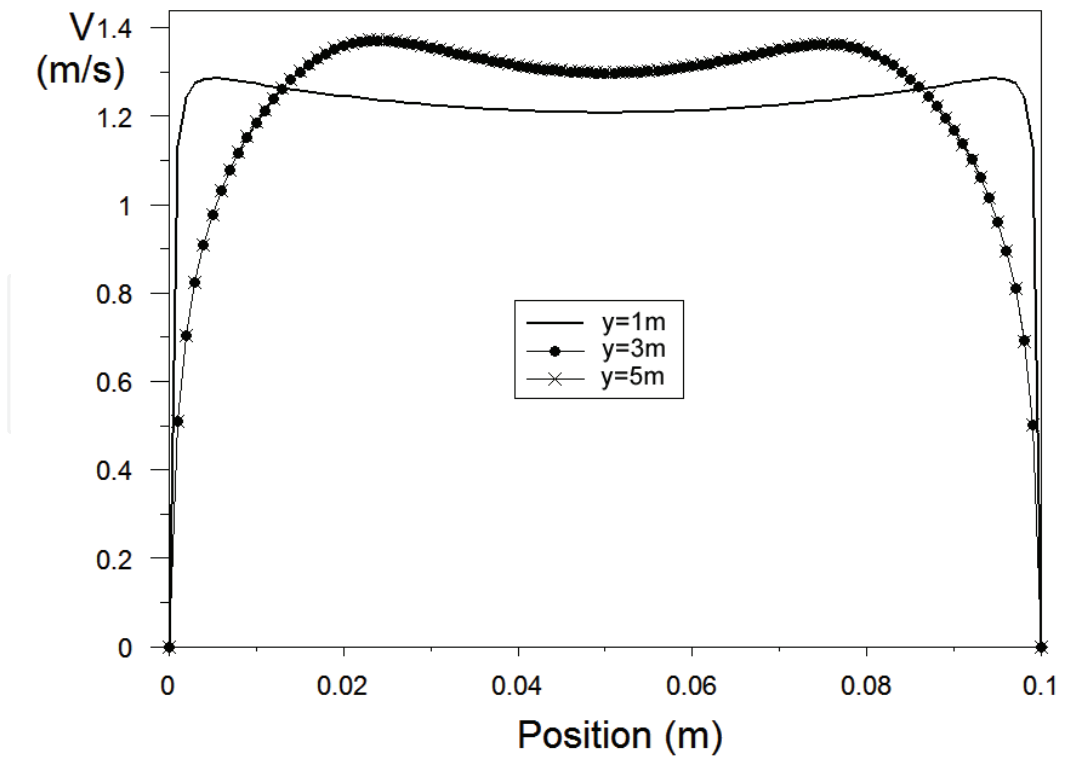


Fig. 10. Facade P2- Velocity profiles ( $L=6$  m,  $d=0.1$  m,  $T_e=301$  K,  $I=400W/m^2$ )



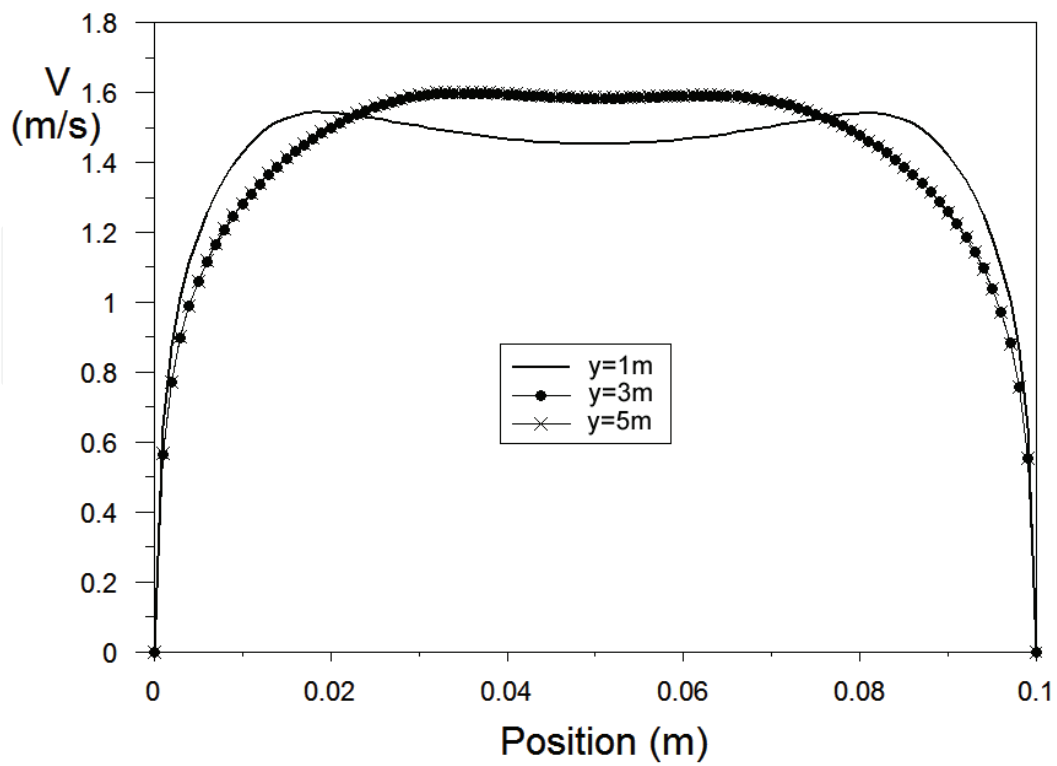


Fig. 11. Facade P3- Velocity profiles ( $L=6$  m,  $d=0.1$  m,  $T_e=301$  K,  $I=400\text{W}/\text{m}^2$ )

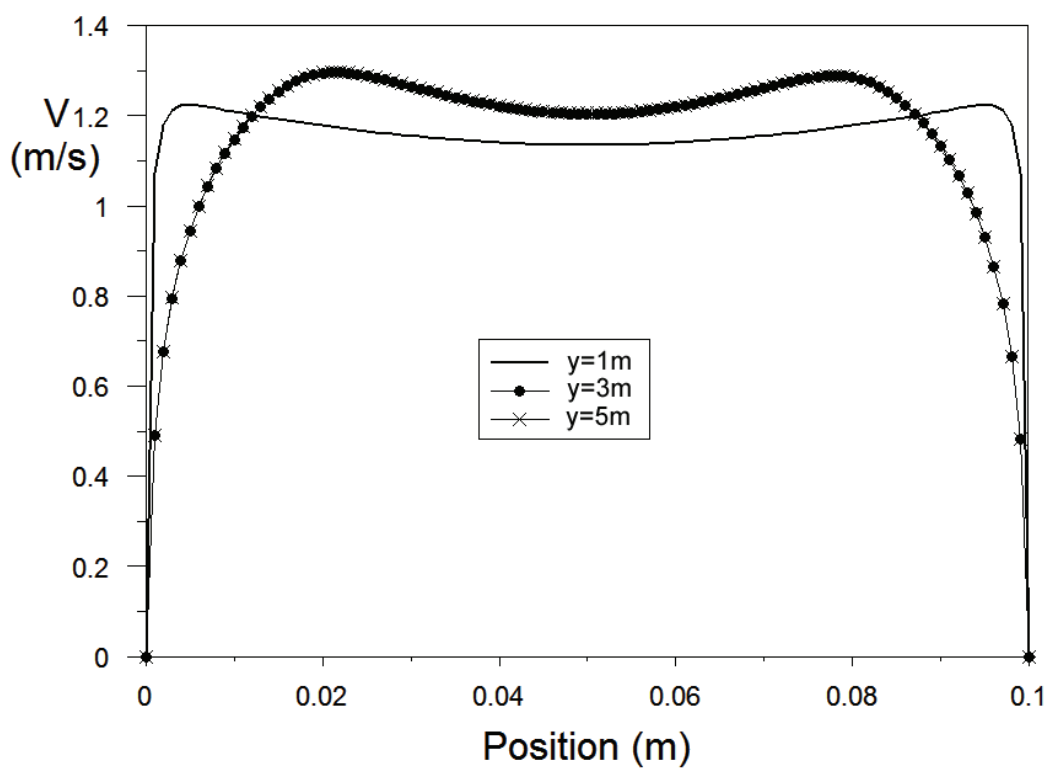


Fig. 12. Facade P4- Velocity profiles ( $L=6$  m,  $d=0.1$  m,  $T_e=301$  K,  $I=400\text{W}/\text{m}^2$ )

The temperature profiles show an increase of the air temperature inside the cavity along the direction of the motion. It is also possible to observe two temperature boundary layers developed in correspondence of the two slabs.

The fluid temperature decreases gradually moving away from the two surfaces delimiting the ventilated cavity and it reaches the value of undisturbed flow outside the thermal boundary layer.

In the first section of the ventilation duct (1/6 of the total length of the facade), as is possible to see in the profile obtained for  $y=1$  m, the temperature increases above in the part of the duct near the two walls, where viscous dissipation is maximum, while the air in the middle of the channel presents a temperature very close to the entrance value  $T_0$ .

At a distance from the entrance sufficiently high (3/6 of the total length of the facade), the air temperature in correspondence of the centerline increases too. From this section the temperature profile becomes "stable".

The temperature profiles obtained at the third section of the ventilation duct (5 / 6 of the total length of the facade) have the same trend as those obtained for the second section, but with higher overall temperatures.

It is interesting to observe that in the case of the ventilated facade P4, the air flow inside the duct is heated less than the other two studied facades. In fact, for the facade P4 has been obtained the lowest value of air temperature inside the duct.

The distributions of velocity observed in the cases of the walls P1,P2 and P4 show the characteristic trend of internal flows in natural convection.

It is possible to observe the existence of two symmetric boundary layers developed near the two slabs that delimit the ventilated duct. The fluid velocity is zero in correspondence of the two walls (condition of adhesion to the wall) and increases with distance from the surface, until it reaches a maximum value ( $x = 0.02$ m) and then decreases again moving toward the center line ( $x = 0.05$  m).

In the first section of the ventilation duct, as shown by the velocity profiles obtained at the section located at  $y = 1$  m, the air flow is not yet fully developed and it has a lower average speed of about 1 m / s for the wall P1, of 1.2 m / s for the walls and P2 and P4 of 1.5 m / s for the wall P3.

In the case of the wall P3, velocity profiles show a parabolic trend with a maximum speed of 1.6 m/s on the centerline ( $x = 0.05$  m).

## 7.2 Forced ventilation

In the case of forced convection, the action of a mechanical propeller (one or more low power fan) that pushes the air inside the double-ventilated, increasing the effects due to local gradients of density characteristic of simple natural convection, has been simulated by imposing a speed input  $v_0$ .

The other boundary conditions have been imposed coincident with those used to study the motion of air in case of natural convection.

The following figures (from 13 to 16) show the velocity and temperature profiles obtained for the ventilated wall P1, for two different values of inlet velocity, respectively,  $v_0(1) = 1$  m/s and  $v_0(2) = 2$  m/s.

The temperature profiles (see fig. 13 and 14) show a very flattened trend in the middle of the channel with two points of maximum in correspondence to the two slabs. The increase of the velocity  $v_0$ , imposed by the fan, causes both the decrease of the temperature difference between the two sides of the duct and the decrease of the temperature difference between the inlet and outlet cross-sections ( $T_L - T_0$ ). Every way the ventilation heat flux,  $Q_v = \dot{m} c_p (T_L - T_0)$ , augment is caused by the increase of the mass air flow.

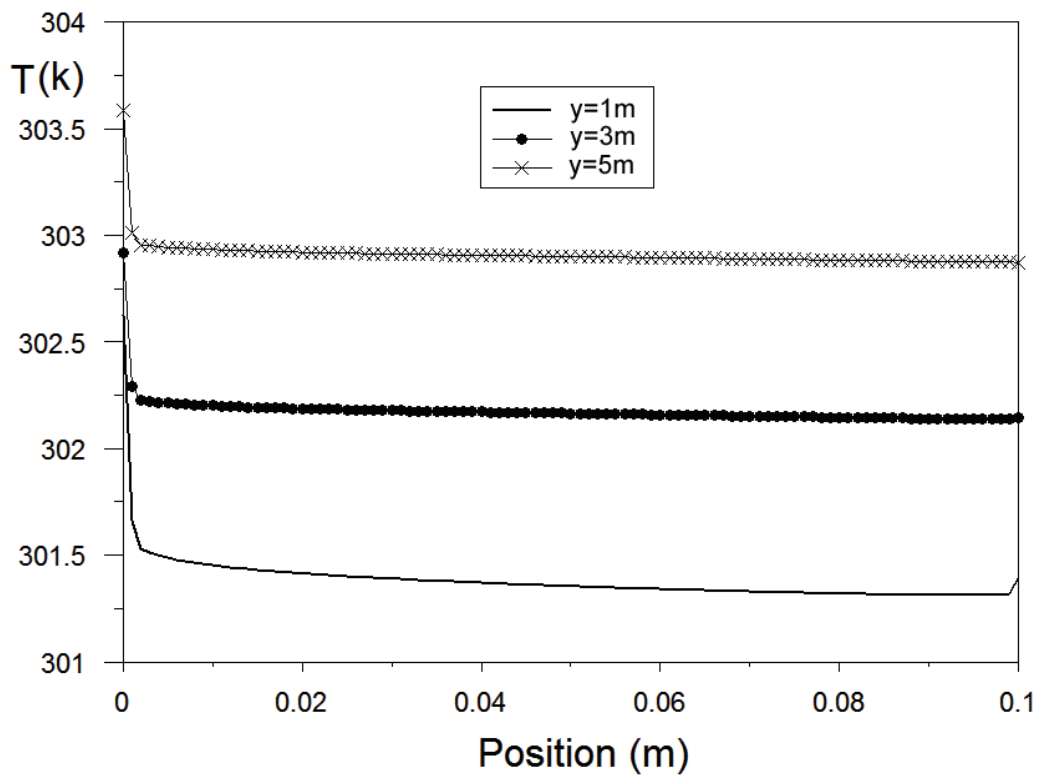


Fig. 13. Facade P1- Temperature profiles ( $L=6$  m,  $d=0.1$  m,  $T_e=301$  K,  $I=400\text{W}/\text{m}^2$ ,  $v_0=1$  m/s)

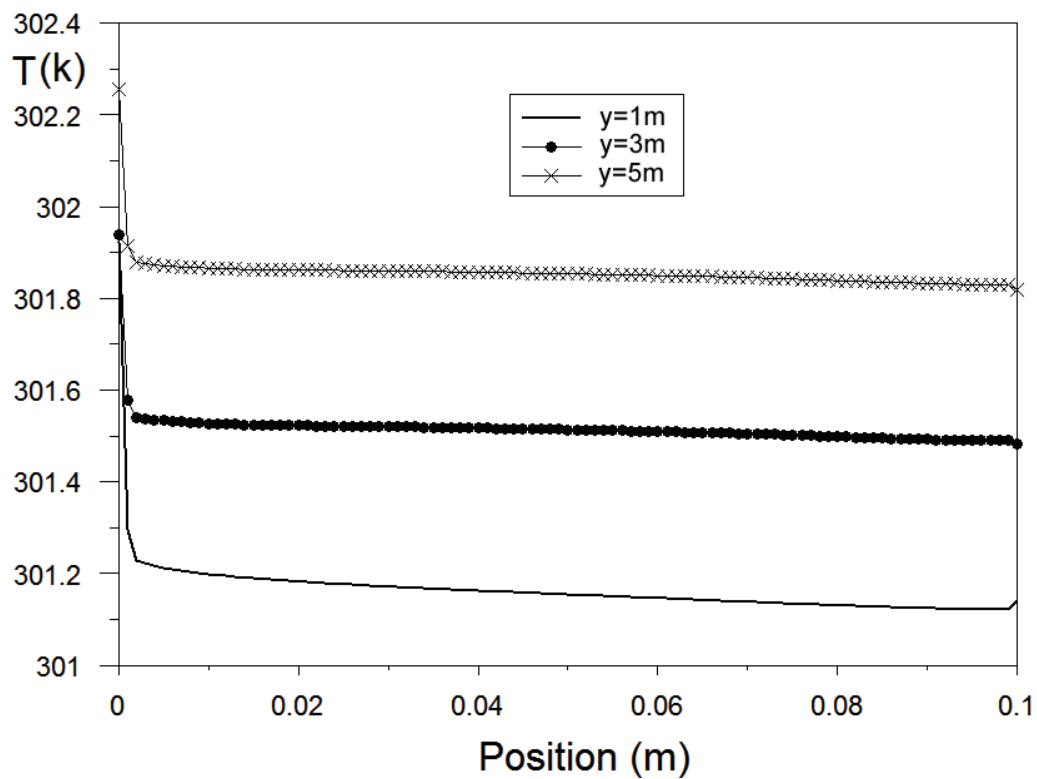


Fig. 14. Facade P1- Temperature profiles ( $L=6$  m,  $d=0.1$  m,  $T_e=301$  K,  $I=400\text{W}/\text{m}^2$ ,  $v_0=2$  m/s)

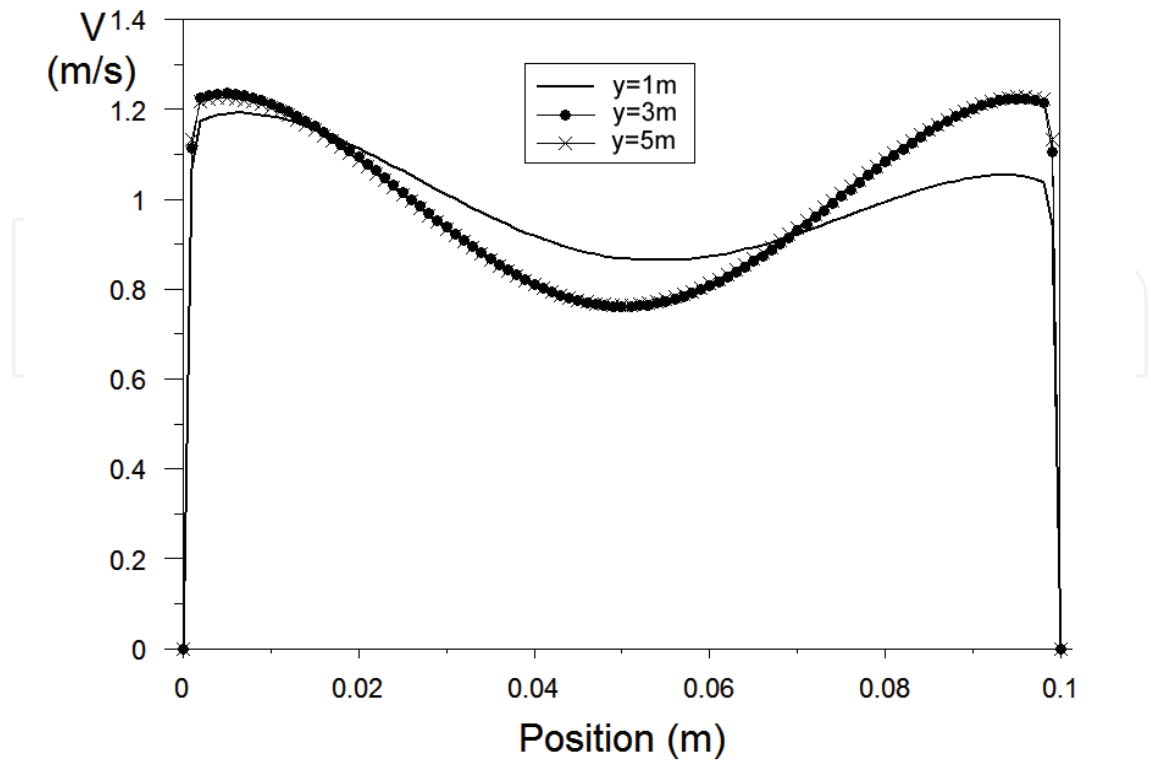


Fig. 15. Facade P1- Velocity profiles ( $L=6$  m,  $d=0.1$  m,  $T_e=301$  K,  $I=400\text{W/m}^2$ ,  $v_0(1) = 1\text{m/s}$ )

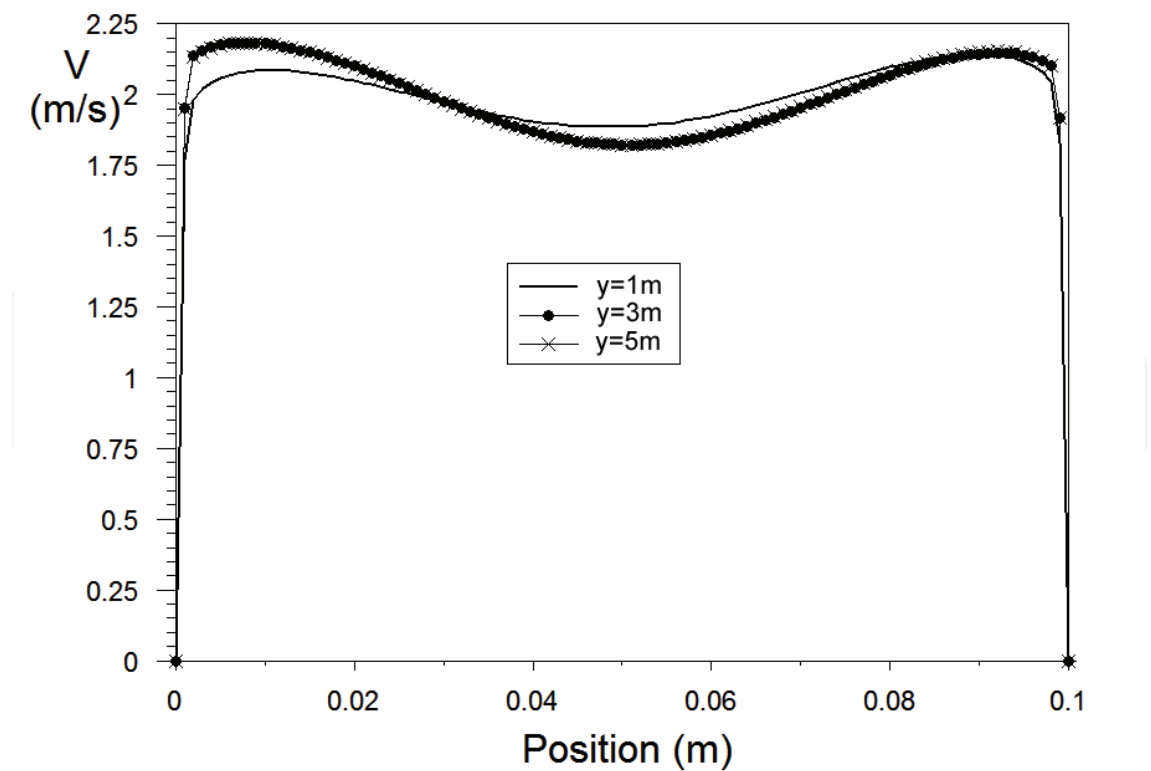


Fig. 16. Facade P1- Velocity profiles ( $L=6$  m,  $d=0.1$  m,  $T_e=301$  K,  $I=400\text{W/m}^2$ ,  $v_0(1) = 2\text{m/s}$ )

The values of temperature inside the channel,  $T_m$ , are less than the ones calculated for lower inlet velocities, consequently it implies the decrease in the heat flux incoming into the building expressed by the relation  $Q_{in}=R_{in}(T_m - T_i)$ .

Increasing the inlet velocity (see fig. 15 and 16) from 1 m/s to 2 m/s, the velocity profiles tend to a flattened trend, the airflow feels less the effect of friction and the two boundary layers become very thin.

The same results have been obtained for the other types of facades object of the study.

## 8. Energy performance of ventilated facades

In order to evaluate the benefit that derives from the use of ventilation, have been calculated heat fluxes entering through ventilated structures, both in presence and absence of ventilation.

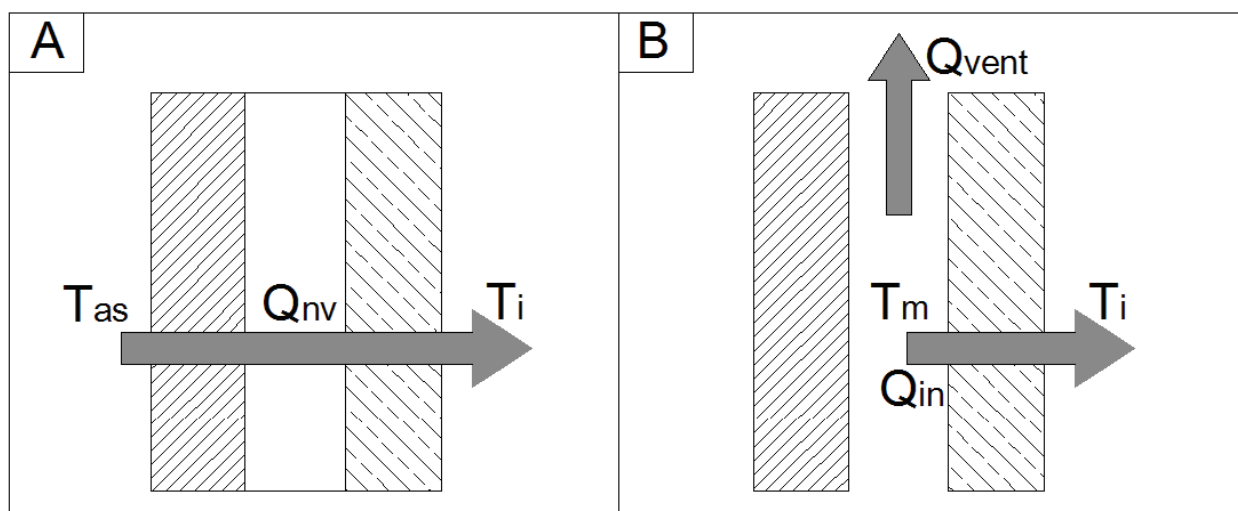


Fig. 17. Heat flux incoming for unventilated(A) and ventilated (B) facade

In the case of lack of ventilation, the incoming heat flux (see fig. 17A) is :

$$Q_{nv} = \frac{T_{as} - T_i}{R_{nv}} \quad (25)$$

where  $T_{as}$  is the temperature-sun-air defined as:  $T_{as} = T_e + aI/h_{oe}$ ,  $T_e$  is the outdoor air temperature;  $a$  is the absorption coefficient of the outer face;  $I$  is the incident solar radiation intensity;  $R_{nv}$  is the thermal resistance of the unventilated facade defined as:

$$R_{nv} = r_i + \sum_i^N \frac{s_i}{\lambda_i} + r_e \quad (26)$$

where  $r_i$  and  $r_e$  are respectively the thermal resistances of the inner and the external surfaces while  $s_i$  and  $\lambda_i$  are the thickness and the thermal conductivity of the  $i^{\text{th}}$  layer (see table 2).

In the case of ventilated facade (see fig. 17B) the heat flux coming into the room will be given by the equation:

$$Q_{in} = \frac{T_m - T_i}{R_i} \quad (27)$$

where  $T_m$  is the average temperature of the air into the duct and  $R_i$  is the total thermal resistance of the internal slab defined as:

$$R_i = r_i + R_A + r_1 \quad (28)$$

where  $r_i$  is the convective thermal resistance of the inner surface,  $R_A$  is the conductive resistance of the internal slab and  $r_1$  is the surface thermal resistance into the duct. The average temperature  $T_m$  inside the duct has been obtained using the values provided by the thermo-fluid simulations and it is expressed by the following empirical formula:

$$T_m = \frac{[zT_1' + (1-z)T_2'] + \frac{T_L + T_0}{2}}{2} \quad (29)$$

where:  $z=R_e/R_{tvo}$  is a dimensionless parameter;  $T_1'$ ,  $T_2'$ , are the air temperatures respectively in correspondence to the two slabs and  $T_L$  the air temperature in correspondence of the outlet section of the duct obtained by the CFD simulations

The CFD simulations under natural convection have been carried out varying both the geometry (the thickness  $d$  of the duct) and the climatic conditions (solar radiation  $I$  and the external temperature  $T_e$ ). For the simulations carried out under mixed convection (natural + forced) has been varied the inlet velocity of air  $v_0$ .

The results of the heat fluxes incoming in presence ( $Q_{in}$ ) and in absence ( $Q_{nv}$ ) of ventilation can be summarized as follows:

- Influence of the width of the duct ( $d$ )

The increase of the width of the ventilated duct  $d$  from 5 cm to 20 cm (see fig.18) provides an improvement of the energy performance of the structure, reducing the thermal loads incoming.

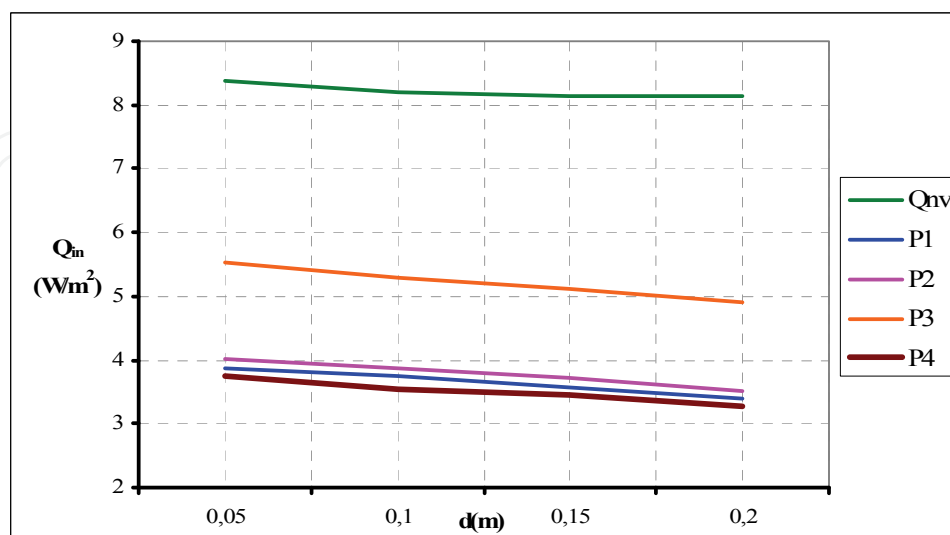


Fig. 18. Variations of heat flux  $Q$  incoming with the width of the duct ( $L=6$  m,  $T_e=301$  K,  $I=400W/m^2$ )

The observed behavior is due to the reduction of relative roughness ( $b/Dh$ ) with the resultant increase in flow rates and ventilation heat load removed from the structure.

The wall P4 results to be the best, while the less efficient results the facade P3.

- Influence of the solar radiation ( $I$ )

The graph in figure 19 shows the heat fluxes entering into the room without ( $Q_{nv}$ ) and in presence ( $Q_{in}$ ) of ventilation varying the incident solar radiation  $I$  from  $100 \text{ W/m}^2$  up to  $600 \text{ W/m}^2$ . It is possible to see that, despite the rise in solar radiation causes the increased heat load incoming ( $Q_{in}$ ), this quantity is always much lower than the heat flux incoming in absence of ventilation ( $Q_{nv}$ ).

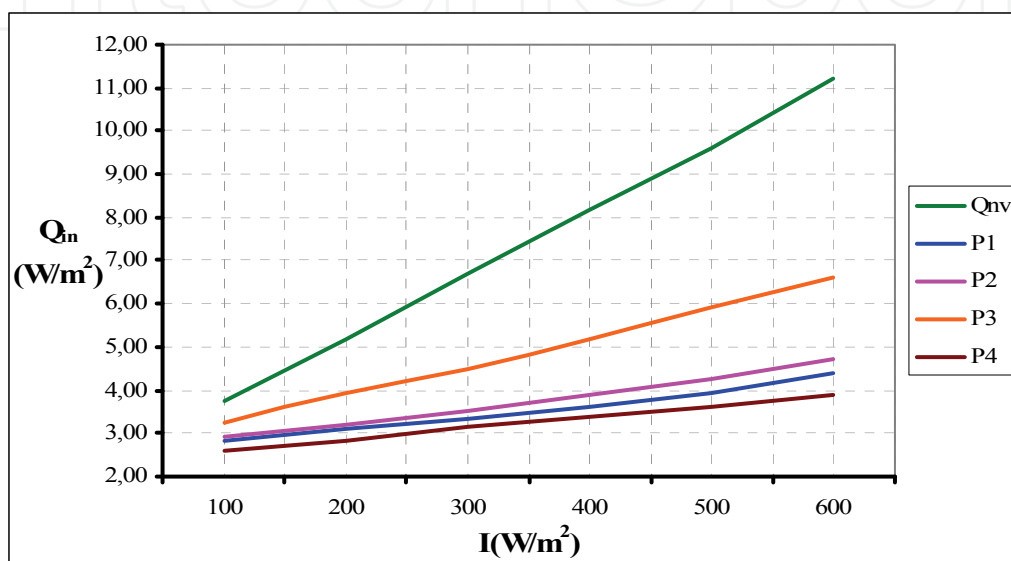


Fig. 19. Variations of heat flux  $Q$  incoming with the solar radiation  $I$  ( $L=6 \text{ m}$ ,  $d=0.1\text{m}$ ,  $T_e=301 \text{ K}$ )

The increase in solar radiation  $I$ , in fact causes a greater heating of the outer wall that feeds the chimney effect in the cavity, allowing to remove a larger amount of heat  $Q_{vent}$  from the structure by ventilation and thereby reducing the heat flux entering the room  $Q_{in}$ . The wall P4 results the best, while the less efficient results the facade P3.

- Influence of the external temperature ( $T_e$ )

The graph in figure 20 shows the behavior of air ventilated cavity at different external temperature  $T_e$  that has been carried out by fixing the incident solar radiation of  $400 \text{ W/m}^2$  and varying the value of the external air temperature  $T_e$ , also coinciding with the inlet temperature  $T_o$ , from  $301 \text{ K}$  up to  $311 \text{ K}$ . The rise in external temperature  $T_e$  causes an increase of the heat load incoming ( $Q_{in}$ ) but this quantity is always lower than the heat flux incoming without ventilation ( $Q_{nv}$ ). This trend is due to the growth of air temperature inside the duct with the consequent increase of heat flux entering in the room  $Q_{in}$ .

It has been possible to observe that, up to  $T_e=306 \text{ K}$ , the facade P4 is the one that uses more efficiently the ventilation, while for  $T_e>306 \text{ K}$  the performances of the four studied facades tend to conform.

For an external temperature  $T_e=311 \text{ K}$ , the heat flux incoming in presence of ventilation assumes a value of about  $10 \text{ W/m}^2$ , however, lower than the heat load entering without the contribution of ventilation.

- Influence of the inlet velocity ( $v_0$ )

Observing the graph in figure 21 is possible to see that the increase of the inlet velocity  $v_0$  causes a decrease of the heat flux incoming  $Q_{in}$  due to the significant augment of the portion of heat load removed by ventilation.

For  $v_0 \geq 2,5$  m/s the heat flux entering the room tends to a horizontal asymptote. This trend is due to the fact that the temperature inside the ventilation duct can not cool down below the outdoor temperature  $T_e$ .

Even in this case the wall P4 results to be the one using more effectively the ventilation, while the P3 wall results to be the one that uses less efficiently the ventilated air gap.

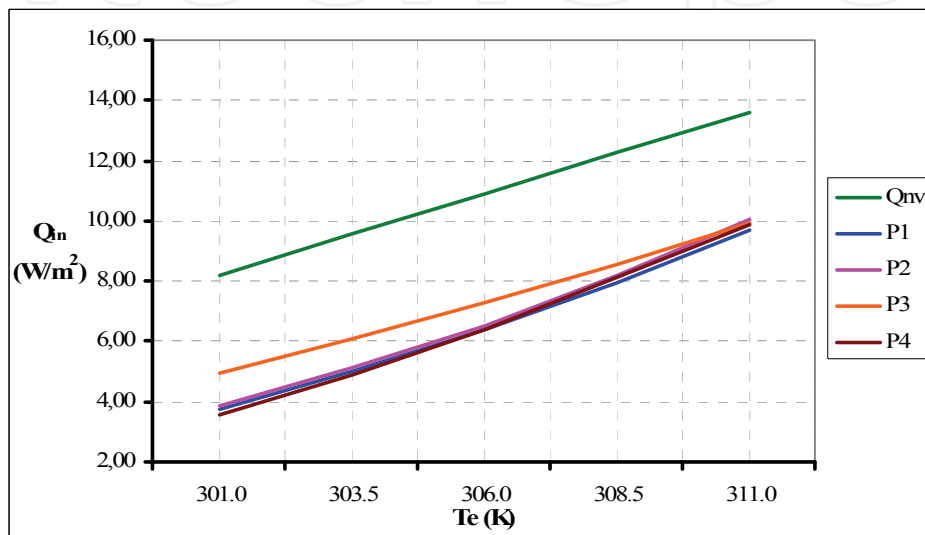


Fig. 20. Variations of heat flux  $Q$  incoming with the external temperature  $T_e$  ( $L=6$  m,  $d=0.1$  m,  $I=400$ W/m<sup>2</sup>)

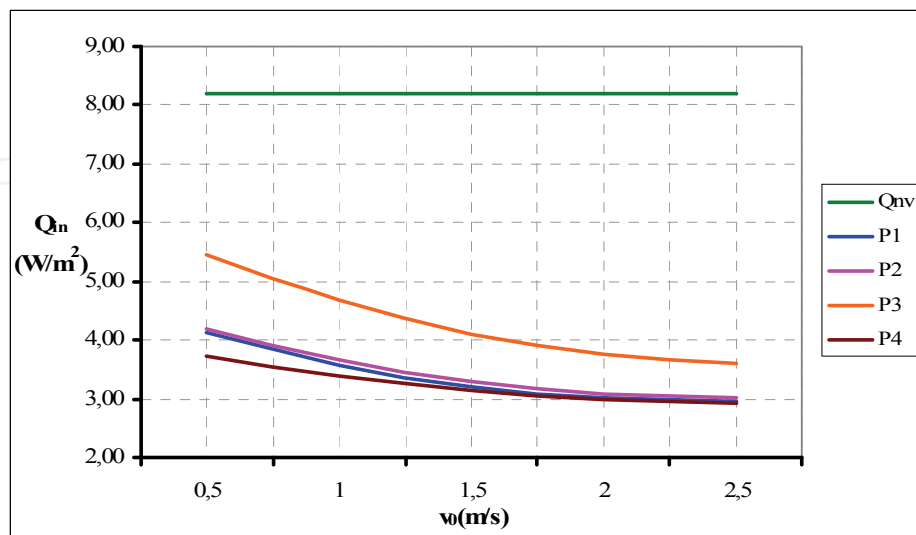


Fig. 21. Variations of heat flux  $Q$  incoming with inlet velocity  $v_0$  ( $L=6$  m,  $d=0.1$ m,  $T_e=301$  K,  $I=400$ W/m<sup>2</sup>)



## 9. Conclusions

A steady calculation method, suitable for design applications, has been illustrated to study the energy performances of ventilated facades during the summer period.

The thermo fluid dynamic behaviour of four different types of ventilated facade, characterized by the same value of the total thermal resistance  $R_{nv}$ , have been examined.

The velocity and temperature profiles have been calculated using the Fluent CFD code, for different values of the width  $d$ , of the duct, incident solar radiation  $I$ , outdoor temperature  $T_e$  and inlet velocity  $v_o$ .

It has been possible to observe significative differences in the velocity and temperature profiles, for each kind of facade, mainly due to the thermo-physics characteristics of the outer facing.

The analysis of the results carried out by the CFD simulations allow the following considerations:

- the heat flux incoming  $Q_{in}$  decreases if the width of the duct  $d$  increases;
- the heat flux incoming  $Q_{in}$  through the facade increases for increasing values of solar radiation  $I$  but the presence of ventilation allows the entry of a minor amount of heat compared to the case in absence of ventilation. Therefore, for constant value of the absorption coefficient  $\alpha$  and the outdoor temperature  $T_e$ , the choice of the ventilated facade is recommended in site with high values of solar radiation  $I$ ;
- the increase of the external air temperature  $T_e$  causes the augment of the heat flux incoming  $Q_{in}$  due to the reduction of the effects of ventilation of the structures;
- the increase of the inlet velocity  $v_o$  causes the reduction of the air temperature inside the duct and consequently of the heat flux incoming  $Q_{in}$ . For  $v_o \geq 2,5$  m/s the heat load entering into the room tends to a horizontal asymptote.

The study has shown that the energy performance of a ventilated facade is influenced by the repartition of thermal resistances between the inner and the outer slabs composing the structure.

The Authors have defined the dimensionless parameter  $z$ , which represents the fraction of thermal resistance facing on the external environment, expressed by the relation:

$$z = R_e / R_{nv} \quad (30)$$

where  $R_{nv}$  is the total thermal resistance of the wall in absence of ventilation and  $R_e$  represents the thermal resistance between the cavity and the external environment, which can be written as follows:

$$R_e = R_A + r_e \quad (31)$$

where  $R_A$  is the thermal resistance of the external coating and  $r_e$  is the laminar external resistance.

It is possible to observe the existence of a correlation between the fraction of thermal resistance  $z$  facing on the outside and the heat fluxes incoming through the ventilated facade  $Q_{in}$ : the wall P4, which is among those analyzed the one that uses more efficiently the ventilation, is characterized by the highest value of  $z$  while the ventilated facade P3 that is the less efficient presents the lowest value of the same coefficient (see fig.22).

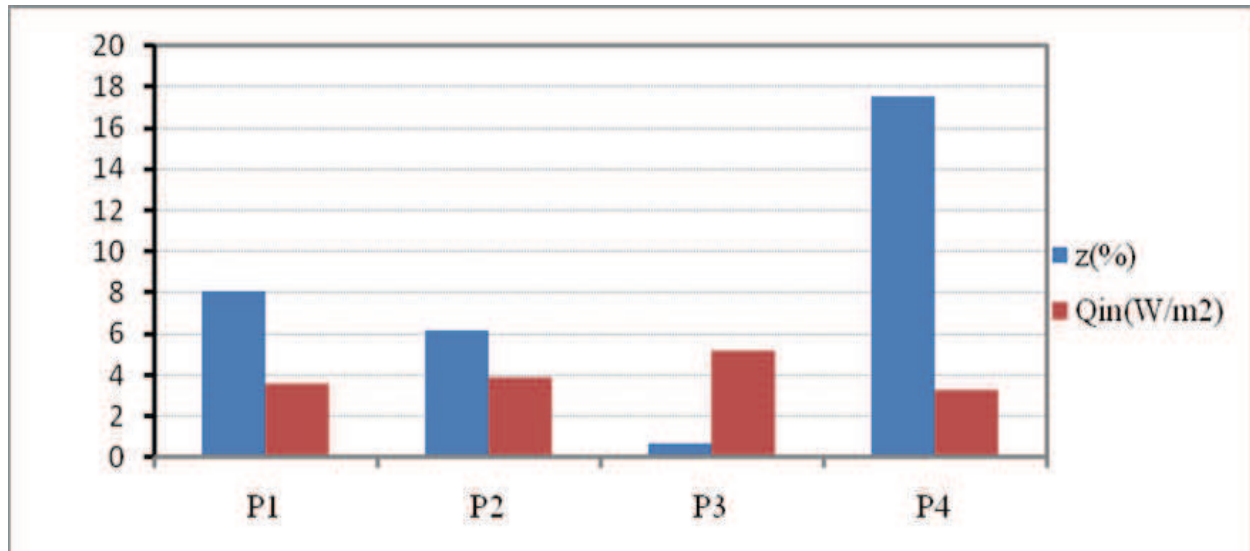


Fig. 22. Comparison between the coefficient  $z$  (%) and the heat flux incoming  $Q_{in}$  ( $T_e=301$  K;  $I=400$  W/m<sup>2</sup>)

It is possible to assert that the ventilated facades, during summer period, achieve high energy performances, with reduction of the heat flux incoming typically above 40%, compared to the same facade unventilated. These energy performances are less advantageous for low values of solar radiation (i.e. facades exposed to the north).

It is considered appropriate to provide the cavity of a system for monitoring the temperature and the velocity of air in order to regulate and optimize the functioning of the ventilated structure.

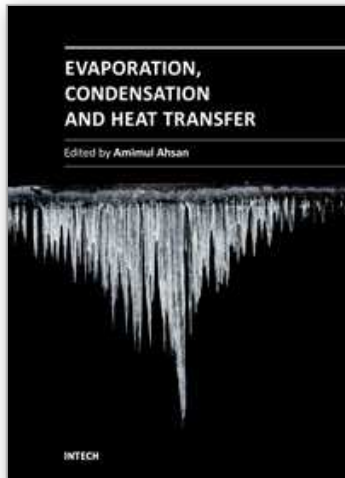
## 10. References

- Balocco, C., Mazzocchi, F., Nistri, P.(2001). Facciata ventilata in laterizio: tecnologia e prestazioni, *Costruire in Laterizio*, n. 83, pp. 63-75 (in Italian).
- Torricelli, M.C.(2000). Caldo d'inverno e fresco d'estate, *Costruire in Laterizio*, 77, pp.56-67 (in Italian).
- Lauder, B.E., Spalding, D.B.(1974). The Numerical Computation of Turbulent Flows, *Computer Methods in Applied Mechanics and Engineering*, n.3, pp.269-289.
- Miyamoto, M., Katoh, Y., Kurima, J., Saki, H.(1986). Turbulent free convection heat transfer from vertical parallel plates, *Heat transfer*, Vol. 4, pp. 1593-1598.
- Fedorov, A. G., Viskanta, R.(1997). Turbulent natural convection heat transfer in an asymmetrically heated vertical parallel-plate channel, *International Journal of Heat and Mass Transfer*, Vol. 40, n. 16, pp. 3849-3860.
- Patankar, S.V.(1980). Numerical heat transfer and fluid flow, *Hemisphere Publications*.
- Rohsenow, W.M., Hartnett, J.P., Gani, E.N. (1985) Handbook of heat transfer fundamentals, 2<sup>nd</sup> ed., McGraw/Hill, New York.
- Patania, F., Gagliano, A., Nocera, F., Ferlito, A., Galesi, A.(2010). Thermofluid- dynamic analysis of ventilated facades, *Energy and Buildings* n.42, pp.1148-1155.
- Patania, F., Gagliano, A., Nocera, F., Ferlito, A., Galesi, A.(2011). Energy Analysis of Ventilated Roof, *Sustainability in Energy and Buildings*, pp. 15-24.

- Ciampi, M., Leccese, F., Tuoni, G. (2002) On the thermal behaviour of ventilated facades and roof, *La Termotecnica*, n.1, pp. 87-97 (in Italian).
- Ciampi, M., Leccese, F., Tuoni, G.(2003). Ventilated facades energy performance in summer cooling of buildings, *Solar Energy*, n.75, 491-502

IntechOpen

IntechOpen



## **Evaporation, Condensation and Heat transfer**

Edited by Dr. Amimul Ahsan

ISBN 978-953-307-583-9

Hard cover, 582 pages

**Publisher** InTech

**Published online** 12, September, 2011

**Published in print edition** September, 2011

The theoretical analysis and modeling of heat and mass transfer rates produced in evaporation and condensation processes are significant issues in a design of wide range of industrial processes and devices. This book includes 25 advanced and revised contributions, and it covers mainly (1) evaporation and boiling, (2) condensation and cooling, (3) heat transfer and exchanger, and (4) fluid and flow. The readers of this book will appreciate the current issues of modeling on evaporation, water vapor condensation, heat transfer and exchanger, and on fluid flow in different aspects. The approaches would be applicable in various industrial purposes as well. The advanced idea and information described here will be fruitful for the readers to find a sustainable solution in an industrialized society.

### **How to reference**

In order to correctly reference this scholarly work, feel free to copy and paste the following:

A. Gagliano, F. Patania, A. Ferlito, F. Nocera and A. Galesi (2011). Computational Fluid Dynamic Simulations of Natural Convection in Ventilated Facades, *Evaporation, Condensation and Heat transfer*, Dr. Amimul Ahsan (Ed.), ISBN: 978-953-307-583-9, InTech, Available from: <http://www.intechopen.com/books/evaporation-condensation-and-heat-transfer/computational-fluid-dynamic-simulations-of-natural-convection-in-ventilated-facades>

**INTECH**  
open science | open minds

### **InTech Europe**

University Campus STeP Ri  
Slavka Krautzeka 83/A  
51000 Rijeka, Croatia  
Phone: +385 (51) 770 447  
Fax: +385 (51) 686 166  
[www.intechopen.com](http://www.intechopen.com)

### **InTech China**

Unit 405, Office Block, Hotel Equatorial Shanghai  
No.65, Yan An Road (West), Shanghai, 200040, China  
中国上海市延安西路65号上海国际贵都大饭店办公楼405单元  
Phone: +86-21-62489820  
Fax: +86-21-62489821

© 2011 The Author(s). Licensee IntechOpen. This chapter is distributed under the terms of the [Creative Commons Attribution-NonCommercial-ShareAlike-3.0 License](#), which permits use, distribution and reproduction for non-commercial purposes, provided the original is properly cited and derivative works building on this content are distributed under the same license.

IntechOpen

IntechOpen